Malaysian Journal of Chemistry, 2025, Vol. 27(3), 306-313
(Special Issue: *International Conference on Sustainable Materials and Technologies, ICSMT 2025*)

Cobalt Incorporation Effects on the Physicochemical Characteristics of NiO Thin Films

Radha Jayalakshmi, V.[1], Pachamuthu, M. P.[2]* and Jeyakumaran, N.[3]*
[1]Department of Physics, E.M.G Yadava Women's College, Madurai, Tamil Nadu 625014, India
[2]Division of Chemistry, School of Sciences, SRM Institute of Science and Technology Tiruchirappalli, Tamilnadu 621105, India
[3]Department of Physics, V.H.N Senthikumara Nadar College, Virudhunagar, Tamil Nadu 626001, India
*Corresponding author (e-mail: jeyakumaran@vhnsnc.edu.in; pachachem@gmail.com)

The main objective of the work is to study the structural, optical, and electronic properties of Cobalt (Co) doped nickel oxide (NiO) thin films synthesised using an efficient chelating approach method. In the present work, 5% Co is doped onto NiO using the sol-gel method with citric acid as a chelating agent and a spin-coated thin film preparation method. The synthesised Co-doped NiO thin film is characterized using Diffuse reflectance spectra (DRS) UV-visible spectroscopy, Fourier transform infrared spectroscopy (FTIR), X-ray diffraction (XRD), and X-ray photoelectron spectroscopy (XPS) techniques. The texture coefficient, Tc(hkl) provides insight into the synthesized thin films crystallographic orientation. O 1s, Ni 2p and Co 2p core-level spectra, of the Co-doped NiO sample were analyzed using the XPS spectra. The O 1s spectra indicated the presence of lattice oxygen, surface hydroxyl groups, and nickel oxides, with a notable reduction in surface hydroxylation at a selected temperature. UV-Visible spectroscopy indicates; thin film thickness is dependent on annealing temperature. Further, Tauc plots of $(\alpha h\nu)^2$ yielded energy band gap values ranging from 3.70 eV for pure NiO to 3.50 eV for 5% Co-doped NiO, indicating a reduction in the band gap with Co doping. This work will impart to the metal oxide layers-based optoelectranic, medical and drug delivery applications.

Keywords: Cobalt doped NiO; thin films; Annealing temperature; Surface morphology; Grain growth

Received: February 2025; Accepted: April 2025

Generally, the transition metal oxides (TMOs) such as manganese oxide (MnO), copper oxide (CuO), cobalt oxide (CoO), iron oxide (FeO), and nickel oxide (NiO) etc., exhibited unique properties, including electrical insulation, antiferromagnetism, and wide bandgap semiconductor behavior, primarily due to their cubic lattice structures and partially filled d-shells. These materials are characterized by their tunable electronic and magnetic properties, which can be influenced by factors such as stoichiometry, synthesis methods, and post-synthesis treatments [1-3]. Moreover, advancements in hybrid functional methods have improved the accuracy of predicting their band gaps, essential for optimizing their use in various technological applications [4]. Overall, TMOs represent a significant area of research due to their versatile functionalities and potential in next-generation technologies [5]. Among the various TMOs, NiO has emerged as a promising p-type oxide, exhibiting significant potential for multifunctional device applications [6]. Due to its wide bandgap (3.6-4.0 eV), NiO exhibits low visible light absorption, suitable for optoelectronic uses [7]. The intrinsic p-type conductivity of NiO is primarily attributed to nickel vacancies (VNi), which serve as acceptor states facilitating efficient hole transport. Studies indicated that in nonstoichiometric NiO, particularly under oxygen-rich conditions, the formation of VNi is energetically favorable, leading to enhanced p-type conduction with conductivity values around 0.1 S/cm in undoped samples [8]. Moreover, the chemical stability and defect tolerance of NiO provide an advantage over n-type TCOs, particularly in harsh environmental conditions [9]. It effectively functions as a hole transport layer (HTL) in perovskite solar cells, improving charge extraction and reducing recombination. These characteristics make NiO suitable for applications in energy conversion, gas sensing, and electrochromic devices. Research indicates that NiO films, when optimized through various deposition techniques such as magnetron sputtering and electron beam evaporation, can achieve high power conversion efficiencies (PCE). For instance, sputtered NiO films treated with sodium periodate improved crystallinity and achieved a PCE of 23.22% in single-junction cells and 30.48% in tandem configurations [10]. Additionally, the incorporation of amino acid-complexed NiO has been shown to reduce interfacial recombination, resulting in efficiencies of 20.27% under ambient conditions [11]. Furthermore, co-doping strategies with Li^+ and Mg^{2+} have also enhanced device performance, achieving efficiencies up to

†Paper presented at the International Conference on Sustainable Materials and Technologies (ICSMT 2025)

16.20% [12]. Overall, these advancements underscore the critical role of NiO in optimizing the execution of perovskite solar cells.

Significant improvements in electroluminescence performance, including an increase in current density (24.5%) and an increase in brightness (84.9%), were observed with the incorporation of cobalt-doped NiO (NiO:Co) compared to traditional ITO anodes. Additionally, the use of lithium-doped NiO films has demonstrated improved electrical properties, which are crucial for efficient hole transport in OLED applications [13]. The development of ultra-smooth NiO-based anodes has led to a 30.6% increase in efficiency for flexible OLEDs, highlighting the importance of surface properties in optimizing device performance [14]. Despite its versatility, challenges remain in optimizing the performance of NiO thin films for advanced applications. The intrinsic resistivity of NiO, typically ranging from 10^{-2} to 10^{-3} Ω·cm, can limit its use as a transparent conducting electrode (TCE) [15]. Achieving higher carrier mobility and lower resistivity without compromising optical transparency requires careful control of material properties through deposition techniques and doping strategies [16]. Researchers have extensively used doping methods to enhance the electrical and optical characteristics of NiO.

The Co-doped NiO thin films, prepared using sol-gel with spin coating, show changes in their structure, light interaction, and electrical behavior depending on the amount of cobalt added and the heat treatment applied. Studies indicate that cobalt doping (1, 3, and 5 at. %) improve the conductivity and decrease the band gap from 3.80 eV to 3.76 eV, with optimal electrical resistivity achieved at 3 at. % Co [16]. The properties are additionally modified by annealing within the 200 °C to 600 °C range, where increased temperatures enhance the material's crystalline structure and lower its band gap down to 2.89 eV [17]. The films maintain high optical transmittance (up to 90%) at lower annealing temperatures, while the morphology transitions from spherical nanoparticles to larger grains with increased temperature [18]. These characteristics position Co-doped NiO films as promising candidates for sensors and opto-electronic applications. Despite efforts, the synthesis of thin films featuring highly doped cobalt within the NiO matrix continues to be a stringent task and needs further investigation. The objective of our study is to explore the influence of Co doping on NiO at 500°C on the variations in NiO thin film properties. Also, the study aims to analyze the chemical states, lattice parameters and bonding states with the help of different instrumentation methods.

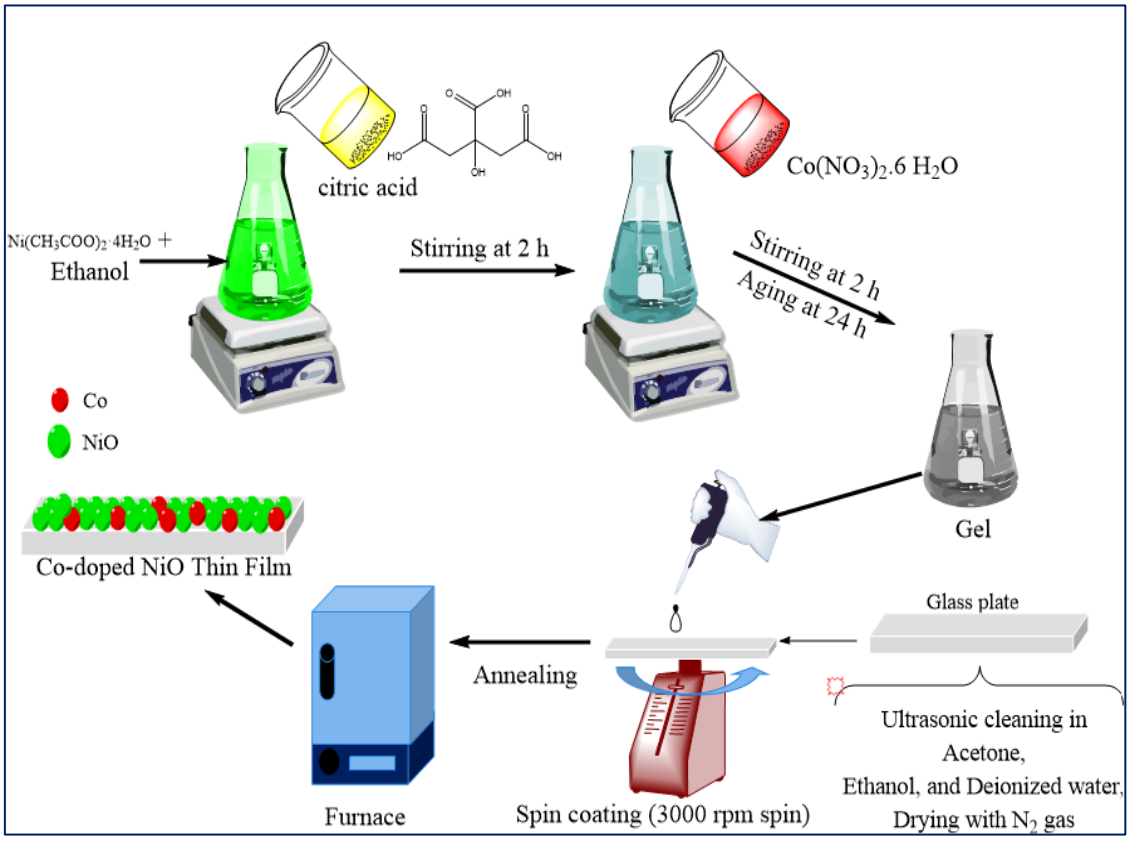

Scheme 1. Steps involved in the Co doped NiO thin film synthesis.

EXPERIMENTAL

Cobalt Doped NiO Thin Film Synthesis

The synthesis of thin film was carried out by adopting the sol-gel method combined with spin-coating methods (Scheme 1), a widely employed technique for producing high-quality thin films. Initially, nickel acetate ($Ni(CH_3COO)_2 \cdot 6H_2O$) and cobalt nitrate ($Co(NO_3)_2 \cdot 6H_2O$) were used as the precursor for NiO, and Co respectively. Initially, a required amount of precursors was dissolved in a mixture of deionized water and ethanol to ensure homogeneity, followed by the addition of citric acid as a complexing agent. To get a clear and stable sol, the solution was constantly mixed for 2 h at a temperature of 30°C. The prepared sol was then aged to improve its viscosity and stability, ensuring uniform film deposition. The spin-coating process was employed to deposit the sol onto cleaned glass substrates. In order eliminate impurities to enhance adhesion, the substrates were carefully cleaned using a number of steps that included acetone, ethanol, and deionized water for deposition. During spin coating, the sol was dispensed onto the substrate, which was then rotated at a speed of 2000 rpm for 40 seconds to spread the solution uniformly. This step was repeated to achieve the desired film thickness. The coated substrates were dried at 100 °C to remove solvents, and then heated at 500 °C for 2 h in a muffle furnace to improve crystallinity and remove organic residues. The obtained sample is denoted as Co-doped NiO.

Characterization Methods

The FTIR method was used to check the bonding of the samples which was recorded on a Bruker instrument with a resolution of 4 cm^{-1} averaged over 100 scans. The texture coefficient is computed to illustrate the favoured alignment of the films through the subsequent formula [16].

$$TC_{hkl} = \frac{I_{(hkl)}/I_{0(hkl)}}{\left(\frac{1}{N}\right)\sum_N I_{(hkl)}/I_{0(hkl)}}$$

Where:

- $Tc_{(hkl)}$ - Texture coefficient for the (hkl) plane
- $I_{(hkl)}$ - Intensity of the (hkl) plane in the sample
- $I_{0(hkl)}$- Intensity of the (hkl) plane in the bulk or standard reference (e.g., JCPDS card)
- N: Number of diffraction peaks considered

The UV-Visible spectroscopy (Thermoscientific Evolution 600 equipment) was used to measure the optical transmittance and determine the bandgap energy using Tauc's method (R).

$$(\alpha h\upsilon)^2 = A(h\upsilon - E_g)$$

where α is the absorption coefficient, hν is the photon energy, A is a constant, and Eg is the bandgap energy. Further, XPS spectrum was measured using an ESA-31 spectrometer with a 180° hemispherical electrostatic analyzer (250 mm radius), capable of 10–500 eV pass energy and 1.5 eV resolution at 5 keV.

RESULTS AND DISCUSSION

XRD Crystallographic Structure of Co Doped NiO Thin Film

The texture coefficients (Tc) for NiO films annealed at 500°C were analyzed for the crystallographic planes (111), (200), (220), (311), and (222). The texture coefficient $Tc_{(hkl)}$ provides insight into the crystallographic orientation of thin films. As shown in Figure 1, the T_c (111) value of 2.7 for the pure NiO film indicates a strong preferred orientation along the (111) plane. In contrast, the T_c values for other planes, such as (200), (220), (311), and (222), were significantly lower, with T_c (200), T_c (220), T_c (311), and T_c (222), signifying suppressed orientations [19]. Further, the variations of TC_{hkl} for pure NiO and Co-doped NiO thin films are compared and given in Figure 1. Notably, $Tc_{(hkl)}$ value equal to 1 indicates a random orientation, where no specific crystallographic plane dominates the film's texture. When $Tc_{(hkl)}>1$, it signifies a desirable orientation along the corresponding (hkl) plane, meaning that this plane is more prominently aligned compared to a randomly oriented sample. Conversely, a $Tc_{(hkl)}<1$ indicates a suppressed orientation along the (hkl) plane, suggesting that this plane is less favourably aligned within the film structure. It is essential to highlight that the doping procedure influenced the preferred alignment. Noticeably, while the undoped NiO film show two dominant development orientations along the (111) and (222) planes, the Co-doped film predominantly exhibits a single preferred growth direction along the (111) plane. The reorientation effect of crystals in a given (hkl) direction due to doping processes is a complex phenomenon influenced by various factors, as evidenced by multiple studies. Luo et al., 2021 have reported that $Pr_{1-x}S_{mx}FeO_3$ single crystals, doping alters the spin reorientation transition temperature (TSR), which is attributed to the competition between Sm^{3+}-Fe^{3+} and Pr^{3+}-Fe^{3+} exchange interactions. This reorientation is crucial for designing spintronic devices, as it affects the magnetic properties significantly [20].

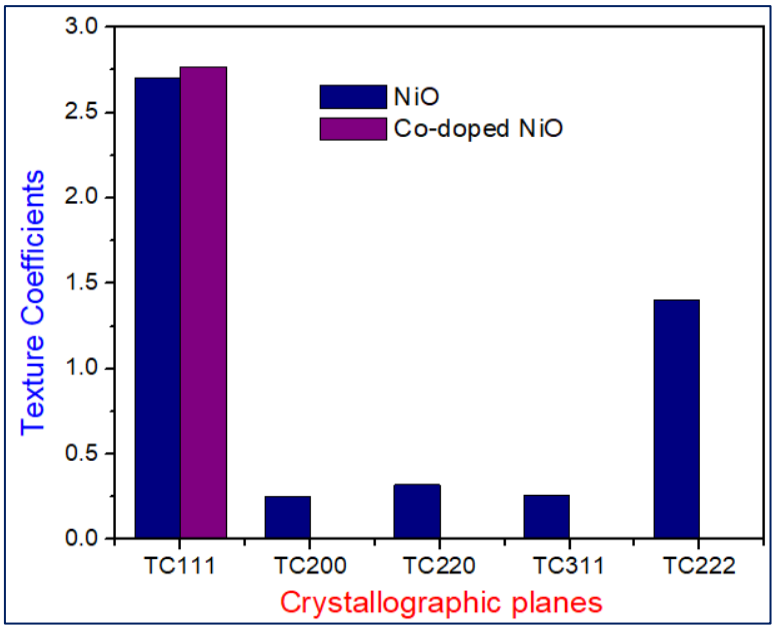

Figure 1. NiO and Co-doped NiO thin films TC and crystallographic planes.

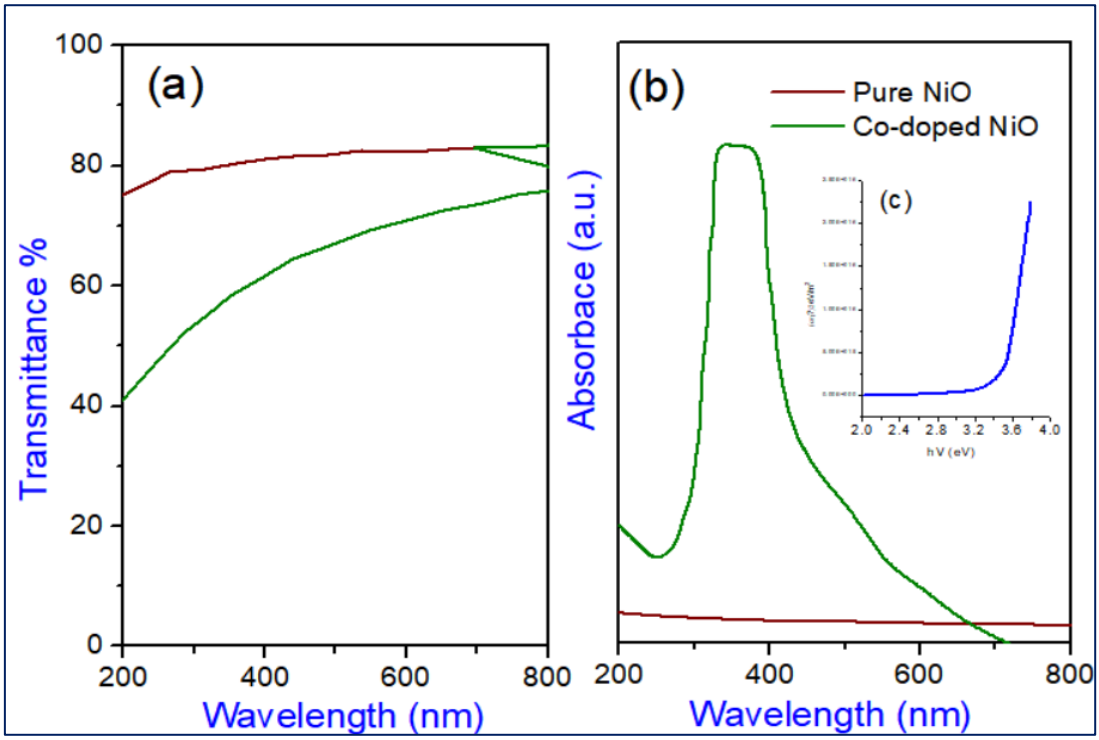

Figure 2. UV-Visible transmittance spectra (a), absorbance spectra of pure NiO and Co-doped NiO thin films (insert - band gap of Co-doped NiO).

Figure 2 shows the transmission and absorbance UV-Visible spectra for pure NiO and Co-doped NiO thin films. As resulting, the transmittance percentage altered due to doping of cobalt on NiO. This can be attributed to the growth in crystallite size linked to the enhanced densification of the film [21-23] and might result from reduced defect scattering. Further, the thickness of thin film is also influenced by annealing temperature. In the prepared state, thin film exhibits amorphous properties. As an outcome of the decrease in unsaturated defects, the amount of localized states also reduced. This improvement in crystallinity and structural arrangement leads to a reduction in the film's thickness [24-25].

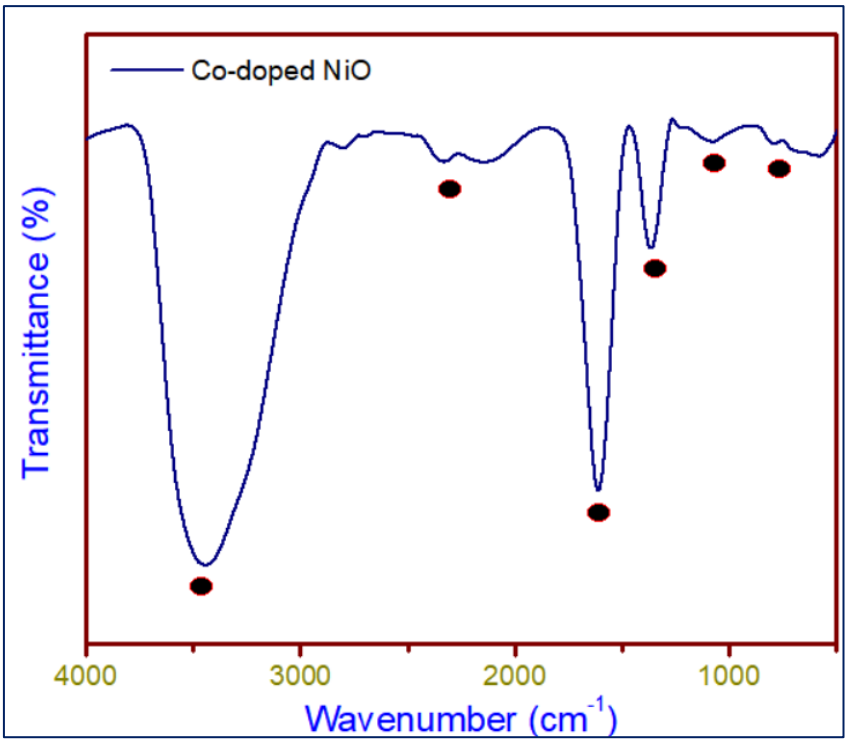

Figure 3. FTIR spectrum of pure Co-doped NiO thin film

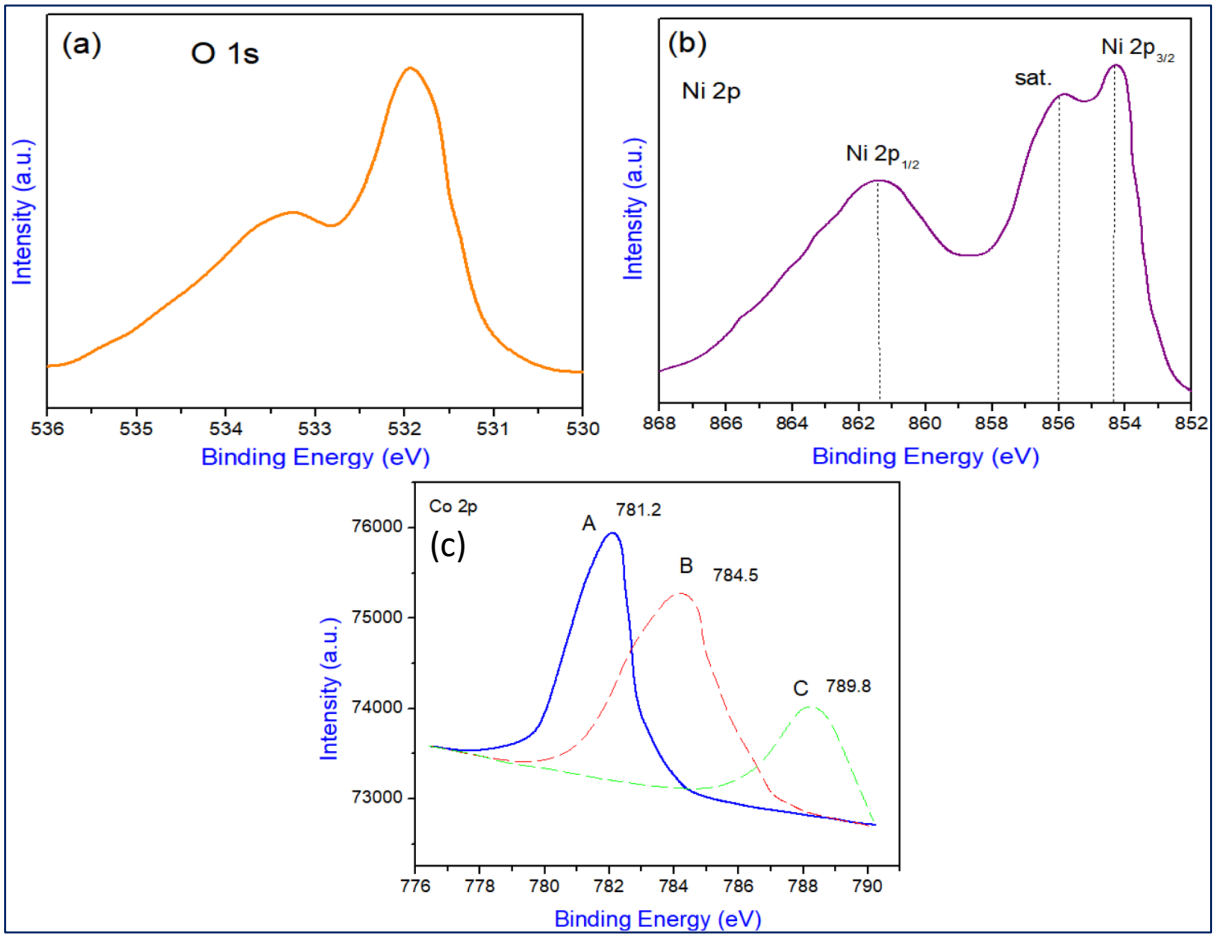

Figure 4. XPS results of (a) O 1s, (b) Ni 2p and (c) Co 2p.

Optical Properties of Co Doped NiO Thin Film using UV Visible Spectroscopy

The Tauc plot of $(\alpha h\vartheta)^2$ with respect to the photon energy ($h\vartheta$) was used to obtain the band gap energy for pure Co-doped NiO. The Tauc plots for Co-doped NiO thin films demonstrate a clear shift in optical band gap energy. A notable trend is observed, Co doped NiO where the band gap decreases from 3.64 eV to 3.50 eV. Remarkably, when the crystal size of a material is reduced to the scale of the exciton Bohr radius or below, quantum confinement takes place. In such small dimensions, the electrons and holes motion is restricted, causing discrete energy levels to form instead of a continuous energy band [26,27]. This confinement effectively increases the band gap by increasing the energy differential between the valence and conduction bands. Due to this phenomenon, the crystallite size decreases and band gap energy increases. A typical phenomenon noticed in annealed direct-transition semiconductor thin films is the reduction in optical band gap energy [28]. The alteration in band gap with Co- doping can be attributed to the change in crystalline quality (growth of larger crystal), as confirmed by the results of XRD analyses.

Co Doped NiO Thin Film Bonding Structure using FTIR

In Figure 3, the FTIR spectrum of Co-doped NiO thin film is depicted. The appearance of the bands at 3400 cm^{-1} and 1650 cm^{-1} confirmed the existence of O–H stretching of residual moisture and hydroxide impurities [29]. The Ni–O stretching band becomes sharper and shifts further to around 450 cm^{-1} and an intense Ni–O stretching peak at 455 cm^{-1}, with minimal presence of hydroxyl band. Further, weak band appears at 560–580 cm^{-1}, corresponding to the formation of Co–O bonds [30]. Analysis confirms the presence of Ni-O, Co-O, and O-H bonds as the main constituents of the Co-doped NiO.

Oxidation States and Elemental Analysis in Co Doped NiO Thin Films using XPS

Figure 4 (a-c) shows the O1s, Ni2p and Co2p XPS spectrum of Co-doped NiO. Figure 4 (a) displays the O1s spectrum of 5% Co-doped NiO films with characteristic main peaks: peak A at 530.37 eV, associated with NiO, and peak B at 532.28 eV, linked to Ni–OH bonds. The increase in BE with Co doping indicates enhanced interaction between Co and oxygen atoms in the NiO lattice. Besides, the peak centered at approximately 530.0 eV is due to NiO lattice oxygen, whereas the peaks around 531.5 eV and 533.0 eV are associated with Ni_2O_3 and surface hydroxyl groups (NiO(OH)), respectively. Moreover, the peak at 532 eV highlights the presence of surface impurities, including carbon-based oxides and hydroxyl groups (H-O-H) formed from residual water molecules [31, 32]. Further, the XPS spectrum (Figure 4(b)) shows the presence of Ni (2p), which consists of two variants ($2p_{3/2}$ and $2p_{1/2}$) due to spin orbit splitting. The BE of Ni (2p) peaks at 856.33 eV and 867.12 eV for Ni $(2p)_{3/2}$ and Ni $(2p)_{1/2,}$ respectively. At 500°C annealing temperature, satellite peaks are diminishes, and the NiO peaks become sharper, signifying the dominance of Ni^{2+} in a well-ordered NiO lattice. The results of the Ni $2p_{3/2}$ spectrum match well with the investigation of the O 1 s spectrum results. The Co 2p spectrum (Figure 4(c)) reveals characteristic peaks for CoO. The BE for Co $2p_{3/2}$ and Co $2p_{1/2}$ peaks are as follows: Co: 781.2 eV (Co $2p_{3/2}$), 797.02 eV (Co $2p_{1/2}$). The Co 2p peaks confirm the successful incorporation of cobalt into the NiO lattice, with slight shifts in BE indicating increasing interaction strength with higher Co concentrations [33].

CONCLUSION

In this work, pure NiO and Co doped NiO thin films (5% Co) were successfully synthesised with citric acid based chelating approach. We found that the modification in the structural, chemical, and morphological characteristics of NiO thin films were due to cobalt doping. The texture coefficients $Tc\ (hkl)$ for NiO thin films showed a significant dependence on Co doping, reflecting changes in crystallographic orientation and film structure. The (111) plane exhibited the highest $T_c(hkl)$, confirming the preferential c-axis orientation of the NiO thin films, particularly at 500°C. From the Taus plot band gap energy calculated for pure Co-doped NiO is 3.5 eV. Also, XPS investigation confirmed the successful incorporation of cobalt into the NiO lattice, with Co and Ni existing in stable oxidation states. Changes in the binding energies of Ni, O, and Co, provide evidence of a significant interaction between the cobalt dopant and the nickel oxide host. These experimental results underscore the significance of controlled doping properties of NiO thin films, making them suited for energy storage, sensors, and electronic devices applications.

REFERENCE

1. Bhooraram (2024) Synthesis and Advanced Applications of Transition Metal Oxides. *International Journal for Multidisciplinary Research*, **6(5)**, 1.

2. Shrikant, B., Sunita, G. (2024) Chapter 5 Transition metal oxide semiconductor materials: properties and applications.

3. Leonov, I., Leonov, I., Alexey, O., Shorikov, V., Anisimov, I., Igor, A., Abrikosov, Igor, A., Abrikosov (2020) Emergence of quantum critical charge and spin-state fluctuations near the pressure-induced Mott transition in MnO, FeO, CoO, and NiO. *Physical Review B*, **101(24)**, 245144.

4. Peitao Liu, Cesare Franchini, Martijn Marsman, Georg Kresse (2020) Assessing model-dielectric-dependent hybrid functionals on the antiferromagnetic transition-metal monoxides MnO, FeO, CoO, and NiO. *Journal of Physics: Condensed Matter*, **32(1)**.

5. Li Chen, Zhonggang Liu, Zheng Guo, Xing-Jiu Huang (2020) Regulation of intrinsic physicochemical properties of metal oxide nanomaterials for energy conversion and environmental detection applications. *J. Mater. Chem. A*, **8**, 17326–17359.

6. Karishma, Neeti, Tripathi, Ratnesh, K., Pandey, A., Tripathi, K., Asokan, Vishal, Bhushan, Vikas, Sharma (2024) Comparative Analysis of Structural, Optical, and Electronic Properties of Nickel Oxide and Potassium-Doped Nickel Oxide Nanocrystals. *Energy Storage*, **6(8)**.

7. Mohammad, Istiaque, Hossain, Brahim, Aïssa (2024) Electron Beam Evaporated Nickel Oxide Thin Films for Application as a Hole Transport Layer in Photovoltaics. *Processes*, **12(12)**, 2809.

8. Kingsley, O., Egbo, Chinedu, Ekuma, Chao, Ping, Liu, Chao, Ping, Liu, Kin, Man, Yu (2020) Efficient p-type doping of sputter-deposited NiO thin films with Li, Ag, and Cu acceptors. *Physical Review Materials*, **4(10)**, 104603.

9. Mari, Napari, Tahmida, N., Huq, Tuhin, Maity, Daisy, Gomersall, Kham, M., Niang, Armin, Barthel, Juliet, E., Thompson, Sami, Kinnunen, Kai, Arstila, Timo, Sajavaara, Robert, L., Hoye, Z., Andrew, J., Flewitt, Judith, L., MacManus-Driscoll (2020) Antiferromagnetism and p-type conductivity of nonstoichiometric nickel oxide thin films. *InfoMat*, **2(4)**, 769–774.

10. Jin, Y., Feng, H., Li, Y., Zhang, H., Chen, X., Zhong, Y., Zeng, Q., Huang, J., Weng, Y., Yang, J., Tian, C., Zhang, Q., Xie, L., Wei, Z. (2024) Recrystallizing Sputtered NiOx for Improved Hole Extraction in Perovskite/Silicon Tandem Solar Cells. *Advanced Energy Materials*, **15(10)**, 2403911.

11. Dilpreet, Singh Mann, Sakshi Thakur, Sushil, S., Sangale, Kwang-Un, Jeong, Sung-Nam Kwon, Seok-In, Na (2024) Interfacial Engineering of Nickel Oxide-Perovskite Interface with Amino Acid Complexed NiO to Improve Perovskite Solar Cell Performance. *Small*, **20**, 2405953.

12. Jia Dong, Shuaibing Guo, Zhaokai He, Zhe Jiang, Jinbiao Jia (2024) Solvent management and Li+/Mg2+ co-doping enable efficient n-i-p NiOx-based perovskite solar cells. *Journal of Solid-State Chemistry*, **339**, 124948.

13. Su-Hua Yang, Hung-Yu Lin, Hih-Chieh Ho, Jyun-Hao Guo (2024) Enhancing OLED electroluminescence by surface modification and work function adjustment of anode through NiO: Co coating. *Optical Materials*, **154**, 115773.

14. Victor Hugo, López-Lugo, Manuel García-Hipólito, Arturo Rodríguez-Gómez, Juan Carlos Alonso-Huitrón (2023) Fabrication of Li-Doped NiO Thin Films by Ultrasonic Spray Pyrolysis and Its Application in Light-Emitting Diodes. *Nanomaterials*, **13(1)**, 197.

15. Yu Bai, Ya-Hui Chuai, Yingzhi Wang, Yang Wang (2022) Ultra-Smooth and Efficient NiO/Ag/NiO Transparent Electrodes for Flexible Organic Light-Emitting Devices. *Micromachine*s, **13(9)**, 1511.

16. Meriem, Touati, T., Boucherka, A., Barbadj, N., Brihi, Fayçal, Labreche (2023) Low resistivity and transparent Co-doped NiO thin films synthesized by the sol-gel method: Structural, morphology and photoluminescence studied for optoelectronic applications. *Optical Materials*, **143**, 114235.

17. Aswathy, R. N., Jiji Varghese, Vinodkumar, R., (2020) Effect of annealing temperature on the structural, optical, magnetic and electrochemical properties of NiO thin films prepared by sol–gel spin coating. *Journal of Materials Science: Materials in Electronics*, **19**, 16634–16648.

18. Tatyana, I., Antoaneta, H., Shipochka, M., Petko, Vitanov (2022). Nickel Oxide Films Deposited by Sol-Gel Method: Effect of Annealing Temperature on Structural, Optical, and Electrical Properties. *Materials*, **15(5)**, 1742–1742.

19. Khan, M. Y., Akhtar, M. Y., Ali Khan, M. F., Abbass, Z., Fayyaz -ur- Rasheed, Saquib Ali, M., Pirzada, N., Ahmed, R. S. (2024) Study of the effects of heating on the physical, optical, and electrical properties of NiO thin films synthesized using a low-cost sol-gel method. *Mehran University Research Journal of Engineering and Technology*, **43(3)**, 150.

20. Luo, X., Rubin, M., Li, Xiaoxuan, Ma, Yunke, Chen, Baojuan, Kang, Jincang, Zhang, Wei, Ren, Zhenjie, Feng, Shixun, Cao (2021) Doping tuned spin reorientation and spin switching in praseodymium-samarium orthoferrite single crystals. *Journal of Physics: Condensed Matter*, **33(27)**, 275803.

21. Tsung-Ming Tsai, Chun-Chu Lin, Wen-Chung Chen, Cheng-Hsien Wu, Chih-Cheng Yang, Yung-Fang Tan (2020) Utilizing compliance current level for controllability of resistive switching in nickel oxide thin films for resistive

random-access memory. *Journal of Alloys and Compounds*, **826**, 154126.

22. Sharma, R., Acharya, A., Moghe, S., Shrivastava, S. B. Gangrade, M., Shripathi, T., Ganesan, V. (2014) Effect of cobalt doping on microstructural and optical properties of nickel oxide thin films. *Materials Science in Semiconductor Processing*, **23**, 42–49.

23. Gomaa, M. M., Reza Yazdi, M., Rodner, M., Greczynski, G., Boshta, M., Osman, M. B. S., Khranovskyy, V., Jens Eriksson, Rositsa Yakimova (2018) Exploring NiO nanosize structures for ammonia sensing. *Journal of Materials Science: Materials in Electronics*, **29(3)**.

24. Hajakbari, F., Afzali, M. & Hojabri, A. (2017) Nanocrystalline Nickel Oxide (NiO) Thin Films Grown on Quartz Substrates: Influence of Annealing Temperatures. *Acta Physica Polonica A*, **131**, 417–419.

25. Hsu, C. H., Chen, K. T., Huang, P. H., Wu, W. Y., Zhang, X. Y., Wang, C., Liang, L. S., Gao, P., Qiu, Y., Lien, S. Y., Su, Z. B. (2020), Effect of Annealing Temperature on Spatial Atomic Layer Deposited Titanium Oxide and Its Application in Perovskite Solar Cells, *Nanomaterials,* **10(7),** 1322.

26. Chougule, M. A., Pawar, S. G., Godse, P. R. (2021) Retraction Note to: Sol–gel derived Co_3O_4 thin films: effect of annealing on structural, morphological and optoelectronic properties. *Journal of Materials Science: Materials in Electronics*, **32**, 24584.

27. Yang, S., Liu, Y., Zhang, Y., Mo, D. (2010) Investigation of annealing-treatment on structural and optical properties of sol-gel-derived zinc oxide thin films. *Bull Mater Sci.*, **33**, 209–214.

28. Patil1, V., Pawar, S., Chougule, M., Godse, P., Sakhare, R., Sen, S. and Joshi, P. (2011) Effect of Annealing on Structural, Morphological, Electrical and Optical Studies of Nickel Oxide Thin Films. *Journal of Surface Engineered Materials and Advanced Technology*, **1**, 35–41.

29. Pachamuthu, M. P., Baskaran, S., Manivannan, C., Kishore, S. C., Bellucci, S., Boopathy, R. (2021) Cobalt Oxide on a Nanoporous TUD-1 Catalyst for Methylene Blue Dye Interaction DFT Studies and Degradation. *Symmetry*, **13**, 1754.

30. Haq, S., Abbasi, F., Ben, A. M., Hedfi, A., Mezni, A., Rehman, W., Waseem, M., Khan, A., Shaheen, H., (2021) Green synthesis of cobalt oxide nanoparticles and the effect of annealing temperature on their physiochemical and biological properties. *Materials Research Express*, **8**.

31. Feldl, J., Budde, M., Tschammer, C., Bierwagen, O., Ramsteiner, M. (2020) Magnetic characteristics of epitaxial NiO films studied by Raman spectroscopy. *J. Appl. Phys.*, **127**, 235105.

32. Cao, L., Wang, D., Wang, R. (2014) NiO thin films grown directly on Cu foils by pulsed laser deposition as anode materials for lithium-ion batteries. *Mater. Lett.*, **132**, 357–360.

33. Abdullah, M. A. R., Mamat, M. H., Ismail, A. S., Malek, M. F., Alrokayan Salman, Khan, A., Haseeb, A., Rusop, M. (2016) Preparation of nickel oxide thin films at different annealing temperature by sol-gel spin coating method. *AIP Conf. Proc.*, **1733**, 020013.

List of captions

Scheme 1. Synthesis of Cobalt doped NiO thin films

Figure 1. TC and crystallographic planes of NiO and Co-doped NiO

Figure 2. UV-Visible transmittance spectra (a), absorbance spectra of pure NiO and Co-doped NiO thin films (insert - band gap of Co-doped NiO)

Figure 3. FTIR spectrum of pure Co-doped NiO thin film

Figure 4. XPS results of (a) O 1s, (b) Ni 2p and (c) Co 2p